PAPER

Check for updates

Quantifying the impact of relative humidity on human exposure to gas phase squalene ozonolysis products†

Pascale S. J. Lakey, [ID] *[a] Andreas Zuend, [ID] [b] Glenn C. Morrison, [ID] [c] Thomas Berkemeier, [ID] [d] Jake Wilson,[d] Caleb Arata,[e] Allen H. Goldstein, [ID] [e] Kevin R. Wilson, [ID] [f] Nijing Wang, [ID] [g] Jonathan Williams,[g] Jonathan P. D. Abbatt [ID] [h] and Manabu Shiraiwa [ID] *[a]

Squalene is a major skin oil lipid which can react with ozone forming a range of products including carbonyls, carboxylic acids, hydroxy ketones, secondary ozonides and hydroperoxides. Previous experimental studies have shown that the yield of these products depends on relative humidity. A new mechanism is developed which treats the reaction of ozone with carbon–carbon double bonds and the subsequent reactions of the Criegee intermediates forming a range of products in both condensed and gas phases. The mechanism is included in kinetic models for a variety of ozonolysis reaction systems including pure squalene particles, squalene and skin oil films, clothing, and skin covered by clothing. The models reproduce experimental measurements reasonably well using relatively consistent parameters, providing insights into the important reactions and processes controlling the concentrations of different species. In general, gas-phase secondary carbonyl product concentrations increase significantly as a function of relative humidity due to their formation from the reaction of Criegee intermediates with water, while carboxylic acids and hydroxy ketone concentrations decrease. For example, human exposure to gas-phase 6-methyl-5-hepten-2-one can increase by approximately a factor of two as the relative humidity increases from 10% to 95%. The model can also reproduce the decay of carboxylic acids in skin oil due to their reaction with Criegee intermediates. Discrepancies between some of the measurements and model outputs indicate that in addition to impacting chemistry, relative humidity may affect other processes such as partitioning to surfaces and condensed-phase diffusion.

Environmental significance

We developed new models that quantify the extent to which relative humidity can impact gas-phase squalene ozonolysis product concentrations indoors. We demonstrate that changing relative humidity can change exposure to some products by more than a factor of two. The models can be used to extrapolate to different indoor conditions to estimate human exposure of ozonolysis products which are known to be skin and respiratory irritants.

[a]Department of Chemistry, University of California, Irvine, CA 92697, USA. E-mail: pascalelakey@gmail.com; m.shiraiwa@uci.edu

[b]Department of Atmospheric and Oceanic Sciences, McGill University, Montreal, Quebec, Canada

[c]Department of Environmental Sciences and Engineering, University of North Carolina, Chapel Hill, NC, USA

[d]Multiphase Chemistry Department, Max Planck Institute for Chemistry, Mainz, Germany

[e]Department of Environmental Science, Policy and Management, University of California, Berkeley, USA

[f]Chemical Sciences Division, Lawrence Berkeley National Laboratory, CA, USA

[g]Air Chemistry Department, Max Planck Institute for Chemistry, Mainz, Germany

[h]Department of Chemistry, University of Toronto, ON, Canada

† Electronic supplementary information (ESI) available. See DOI: https://doi.org/10.1039/d2ea00112h

Introduction

Human skin oils present on clothing and skin are composed of approximately 10% squalene, which has six double bonds and is therefore highly reactive towards ozone.[1] The reaction of ozone with squalene leads to a variety of gas- and condensed-phase products including carbonyls, carboxylic acids, hydroxy ketones, secondary ozonides and hydroperoxides.[2–6] Many of the gas-phase ozonolysis products have previously been quantified when soiled clothing or people have been exposed to ozone in laboratory chambers.[5,7–11] Some of the products are known to be skin and respiratory irritants and have been linked to clogged pores, inflammatory acne, possible wrinkling of the skin and DNA damage.[12–22] It is therefore important to be able to quantify them. Recent experimental measurements of squalene

© 2023 The Author(s). Published by the Royal Society of Chemistry

Environ. Sci.: Atmos., 2023, **3**, 49–64 | 49

ozonolysis products in the condensed and gas phases have shown that their concentrations are impacted by relative humidity (RH).[23,24] These studies have also demonstrated that the ratio of volatile and semi-volatile products to non-volatile products increases significantly with RH.[23,24] Similar trends have been observed when soiled clothing has been exposed to ozone at different RH in chambers.[7,24] These observations are likely explained by the reaction of Criegee intermediates (CIs) with water forming carbonyl species, while at lower RH non-volatile secondary ozonides form.[23,25] Additional experiments have demonstrated that acids, which are present in skin oils at high concentrations, can react with CIs forming hydroperoxides.[2,26]

The concentrations of squalene ozonolysis products will be highly dependent on indoor conditions.[6] Chemistry indoors is affected by conditions which can vary significantly in many ways, including variations in temperature, RH, room size, indoor surfaces, occupancy, indoor activities, air exchange rates, ventilation strategies, light levels, outdoor pollutant levels that are transported indoors, and oxidant concentrations.[27–30] Due to the complexity of indoor environments, the fact that people spend most of their time indoors and the impact that indoor air can have on outdoor chemistry,[31] it is important to develop models to improve our understanding of indoor chemistry. Indoor chemistry models can be used to better understand current experimental measurements, extrapolate to different indoor conditions and uncover gaps in our current understanding of indoor chemistry.[32] Several models have recently been developed to examine the reactions of ozone with squalene; the chemistry in these models is usually highly simplified and tend to concentrate on carbonyl products,[23,33–38] while Heine *et al.*[23] treated complex chemistry to model the bulk phase products of pure squalene particles as a function of ozone exposure and RH.
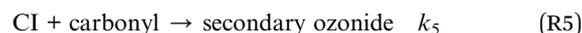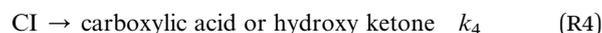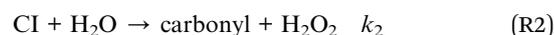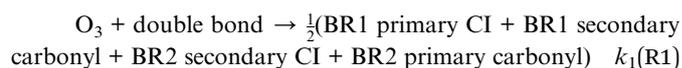
We previously developed the kinetic multilayer model of surface and bulk chemistry of the skin and clothing (KM-SUB-Skin-Clothing), which treats squalene ozonolysis reactions in the skin and clothing as well as mass transport of ozonolysis products in the different regions of the skin (skin oil, stratum corneum and viable epidermis).[33,34] Parameters in KM-SUB-Skin-Clothing are based on fundamental physical and chemical processes (adsorption and desorption, Fickian diffusion, partitioning and chemical kinetics) which allows for an in depth understanding of the processes controlling the concentrations of species to be obtained and allows for extrapolation to different scenarios. The chemistry in the original KM-SUB-Skin-Clothing model, however, was highly simplified with an assumption of carbonyls being the only products, without treating chemistry of CIs and impacts of RH. Note that when we mention the impact of RH in this work, we are discussing the effect of changing the water vapor concentration rather than changes in RH caused by varying temperatures. In the current study, we develop a mechanism which treats the reaction of ozone with carbon–carbon double bonds contained in both squalene and its products, the formation of CI and their subsequent reactions. This enables species such as carboxylic acids and hydroxy ketones to be quantified in the gas phase and

the effect of RH on the squalene ozonolysis product distribution to be estimated for different scenarios. We include this mechanism in kinetic models for different reaction systems including ozonolysis of pure squalene particles, ozonolysis of squalene and skin oil films, and ozone exposure to human occupants. We also model the reaction of acids contained in skin oils with CI, which may eventually help in determining the fate of these species.[4]

Model description

Development of the squalene ozonolysis chemical mechanism

The generalized mechanism of squalene ozonolysis included in our models is based on previously published work and shown below.[2,23,39,40] Briefly, it consists of ozone reacting with carbon–carbon double bonds forming both primary and secondary carbonyls and CIs with specific branching ratios (BR). CIs can subsequently react with water, ozone, carbonyls, carboxylic acids or can isomerize.

$$O_3 + \text{double bond} \rightarrow \tfrac{1}{2}(\text{BR1 primary CI} + \text{BR1 secondary carbonyl} + \text{BR2 secondary CI} + \text{BR2 primary carbonyl}) \quad k_1 \text{(R1)}$$

$$CI + H_2O \rightarrow \text{carbonyl} + H_2O_2 \quad k_2 \quad \text{(R2)}$$

$$CI + O_3 \rightarrow \text{carbonyl} \quad k_3 \quad \text{(R3)}$$

$$CI \rightarrow \text{carboxylic acid or hydroxy ketone} \quad k_4 \quad \text{(R4)}$$

$$CI + \text{carbonyl} \rightarrow \text{secondary ozonide} \quad k_5 \quad \text{(R5)}$$

$$CI + \text{carboxylic acid} \rightarrow \text{hydroperoxide} \quad k_6 \quad \text{(R6)}$$

The complete mechanism was fully written out and included in the model and consists of over five hundred reactions as summarized in Table S1.† This mechanism allows every double bond to react with ozone and for all CIs to undergo the reactions (R2–R6). Reactions (R5) and (R6) include the reactions of all CIs with all carbonyls and carboxylic acids that have formed from other reactions. Many of the reactions occur both in the condensed and gas phases as indicated in Table S1.† The structure of a few selected compounds of interest, which are mentioned in the text below, are summarized in Table S2.† Assumptions and simplifications were applied to increase computational efficiency and also because some mechanisms are so poorly understood that they cannot be constrained with confidence. We assume that all carbon–carbon double bonds react with ozone with the same rate coefficient ($k_1 = 2.2 \times 10^{-17}$ cm^3 s^{-1} in the bulk) and that the rate coefficients for CIs (k_2–k_6) are also independent of the specific structures of the reactants. These assumptions could be revisited in the future as theoretical calculations or experimental observations become available. We assume that CIs are short-lived species and therefore do not have time to partition between the gas and condensed bulk phases. If a molecule contains both a CI and another reactive functional group, we assume that the CI will always react first as it is so short-lived. The formation of H$_2$O$_2$ is not explicitly included in this model. We also do not treat any

50 | *Environ. Sci.: Atmos.*, 2023, **3**, 49–64

© 2023 The Author(s). Published by the Royal Society of Chemistry

solvent cage effects of CIs reacting with carbonyls. For simplicity, no interfacial reactions (*i.e.*, reactions involving adsorbed molecules) are included with all reactions occurring in the bulk or gas phases. Note that prior work[41] has indicated that the reacto-diffusive length of ozone in squalene is short, suggesting that in some cases interfacial reactions may impact the kinetics as previously discussed in Heine *et al.*[23] and may also be different to bulk phase reactions. A recent study has shown the importance of surface reactions for the ozonolysis of oleic acid,[42] while another study has elucidated that there will be different concentrations of the various squalene double bonds at the air–oil interface which may have implications for ozone chemistry and the product distribution.[43] While this aspect is beyond the scope of current study, it may warrant further investigations by adding complexity to the model in the future.

We have tried to include the most important reaction pathways in the model based on species that have been observed in measurements. It should be noted that additional reactions may also occur such as auto-oxidation, the decay of secondary ozonides and hydroperoxides and other reactions involving CIs.[3,44,45] Gas-phase chemistry is also known to be complex with different pathways such as the rearrangement of CIs forming OH and vinoxy radicals, and the formation of dioxiranes,[46–48] which are not included in this mechanism. There is also evidence that CIs can form OH and vinoxy radicals during the heterogenous ozonolysis of alkenes.[49] Formed radicals could subsequently react with other molecules. Several studies have observed or predicted that gas-phase ozonolysis reactions can lead to secondary ozonide formation.[50–53] For simplicity, we assume that the gas-phase chemistry mechanism is the same as the bulk-phase chemistry mechanism, but complexity could be added in the future as the reaction pathways and branching ratios for the specific volatile and semi-volatile products in our work become better understood. It should also be noted that the gas-phase chemistry may include heterogeneous reactions occurring on chamber or flow tube surfaces which are not explicitly treated in the models. Finally, as we are mainly interested in quantifying gas-phase products, the mechanism is simplified by treating the two halves of secondary ozonides and hydroperoxides, which may have different functional groups attached to the carbon atoms on either side, individually. By not treating the individual full secondary ozonide and hydroperoxide molecules, and the many different potential combinations of functional groups, we reduce the number of species treated in the model significantly. Note that, although we make this simplification, the concentration of $C_{30,SOZ}$, a secondary ozonide which contains 30 carbons, (see Table S2† for the structure) can be calculated by adding one additional differential equation to the model which treats the six formation reactions of $C_{30,SOZ}$ (CIs reacting with carbonyls) and the loss of $C_{30,SOZ}$ due to ozonolysis.

The complete mechanism is used when modeling squalene particles and squalene and skin oil films. However, it is too computationally expensive to include all reactions in the clothing model and KM-SUB-Skin-Clothing; the mechanism was therefore simplified as shown in Table S1.† Mechanism

simplification was performed by systematically testing the effect of removing certain reaction pathways and products on the evolution of the concentrations of the major gas-phase products. Any reactions that only had a negligible or very small impact on gas-phase products were removed from the mechanism. Reactions may not impact the concentration of gas-phase species significantly if their rate is slow compared to other reactions due to small rate coefficients or low concentrations of reactants. Some reactions that only lead to non-volatile and non-reactive products were also removed. The yield of volatile products from certain reactions was low, allowing these reactions to be removed without impacting their gas-phase concentrations. We do not expect that using the simplified mechanism will impact our conclusions as the focus of this study is simulating gas-phase species.

Modeling the ozonolysis products of pure squalene particles

The kinetic multilayer model of gas–particle interactions (KM-GAP)[54] was applied to reproduce the measurements of Heine *et al.*[23] and Arata *et al.*,[24] which consisted of exposing pure squalene particles to different concentrations of ozone at different RHs. KM-GAP uses a flux-based approach by treating gas-phase diffusion to and from the surface of the particles as well as reversible partitioning into the bulk of the particles and the complete chemical mechanism described above and shown in Table S1.† For simplicity, the bulk of the particles was treated with one well-mixed bulk layer which is relatively consistent with small (∼300 nm) liquid particles. Further sensitivity tests suggested that treating bulk diffusion would have a negligible impact on the model results. The volume of the particles is continuously estimated based on the total volume of the individual molecules present in them. As a further simplification, we assume in this model that for an elemental O : C ratio of zero, no partitioning of water into the particle bulk will occur, which is consistent with thermodynamic predictions by the Aerosol Inorganic–Organic Mixtures Functional groups Activity Coefficient (AIOMFAC) model; see below. Therefore, the O : C ratio is also continuously calculated and is used to determine the equilibrium water gas–liquid partitioning coefficient (K_{H_2O}) at a given temperature as follows:

$$K_{H_2O} = O : C \text{ ratio} \times \beta \qquad (E1)$$

where β is a factor that is determined by AIOMFAC. Species which are treated as volatile, as well as the set of model parameters applied, are summarized in Tables S2 and S3.†

AIOMFAC modeling

The water content and water uptake behavior of a liquid mixture can affect the partitioning of other species as well as the time-scale of diffusive mass transfer. One aspect of this work was to determine potential water uptake of pure squalene as well as how the presence of a mixture of squalene oxidation products may change the expected water uptake after squalene exposure to ozone. We also assessed whether more polar squalene oxidation products may phase-separate from unoxidized

© 2023 The Author(s). Published by the Royal Society of Chemistry

Environ. Sci.: Atmos., 2023, **3**, 49–64 | 51

squalene and similar low-polarity compounds when exposed to higher RH. To this end, we employ a thermodynamic equilibrium model based on the Aerosol Inorganic–Organic Mixtures Functional groups Activity Coefficient (AIOMFAC) model, which treats the nonideal mixing in liquid solutions. The AIOMFAC model and its parameterization and validation are described in detail elsewhere.[55,56] For the applications in this study, we use an AIOMFAC-based gas–particle partitioning and liquid–liquid equilibrium model (AIOMFAC–LLE).[57,58] This model allows for predictions of the RH-dependent equilibrium water content in a specific overall mixture of compounds (here squalene ozonolysis products). Such predictions allow for the characterization of the hygroscopicity of different skin oil proxy systems. They also enable the detection of liquid–liquid phase separation (LLPS) in cases where it is thermodynamically favorable. A system of squalene ozonolysis products considered for water uptake computations is detailed in Table S4.†

Using the AIOMFAC-based equilibrium model, the RH-dependent water uptake of squalene and of a multicomponent mixture of squalene oxidation products were predicted at room temperature (298 K). These predictions allowed a value of β in eqn (E1) to be estimated and used in the kinetic modeling. The thermodynamic model predictions show that pure squalene exhibits a negligible equilibrium water uptake from low to high RH. The mass fraction of water is estimated to be less than 0.003 even at 99.9% RH. This was expected for a nonpolar organic compound and the partitioning coefficient of water into pure squalene was therefore set to 0 in the kinetic model (eqn (E1)). To represent a mixture of squalene plus ozonolysis oxidation products, a surrogate system was introduced. The composition of the surrogate system is listed in Table S4:† the oxidation products and their relative yields were obtained from a kinetic reaction simulation with $T = 298$ K, RH = 70%, and O_3 exposure = 3×10^{15} molecules cm^3 s. The resulting system

contains ~5% unreacted squalene, while the remainder consists of 19 ozonolysis products, each of which contains one or several oxygen-bearing functional groups, such as secondary ozonide and carbonyl groups. Fig. 1a shows the predicted equilibrium water uptake for this system as a function of RH when the organic compounds are assumed to be nonvolatile. The water uptake of this system is larger than that of pure squalene; however, it remains modest with a mass fraction of water of less than 0.05 at 99.9% RH and of approximately 0.026 at 80% RH. This corresponds to a hygroscopicity parameter (κ)[59] of $\kappa \approx 0.008$ at 80% RH. No LLPS was predicted for the case shown in Fig. 1a. We can conclude that the hygroscopicity of early-generation squalene oxidation products is low. It should be noted that a water mass fraction of 0.026 at 80% RH is equivalent to a gas-to-liquid water partitioning coefficient of $\sim 5.8 \times 10^{-2}$ mol cm^{-3} atm with an assumed solution density of 1 g cm^{-3}. The O : C ratio for the products in Table S4† is ~0.32 which resulted in $\beta = 0.18$ mol cm^{-3} atm being used in eqn (E1) for consistency with AIOMFAC. It should also be noted that the partitioning coefficient of water and the rate coefficient $k_{2,bulk}$ are codependent in the kinetic model, as the same model outputs are obtained if one of these parameters is increased by a certain factor while the other parameter is decreased by the same factor.

Modeling the ozonolysis products of thin squalene and skin oil films

A kinetic model was applied to reproduce the measurements of Zhou et al.[2] and Zhou et al.,[4] which consisted of exposing a squalene film or a skin oil film, respectively, to 50 ppb ozone in a flow tube and measuring the relative change in different bulk-phase species over time under dry conditions. KM-GAP is adapted by changing the geometry from particles to a flat layer of squalene or skin oil. An assumption is made that volatile
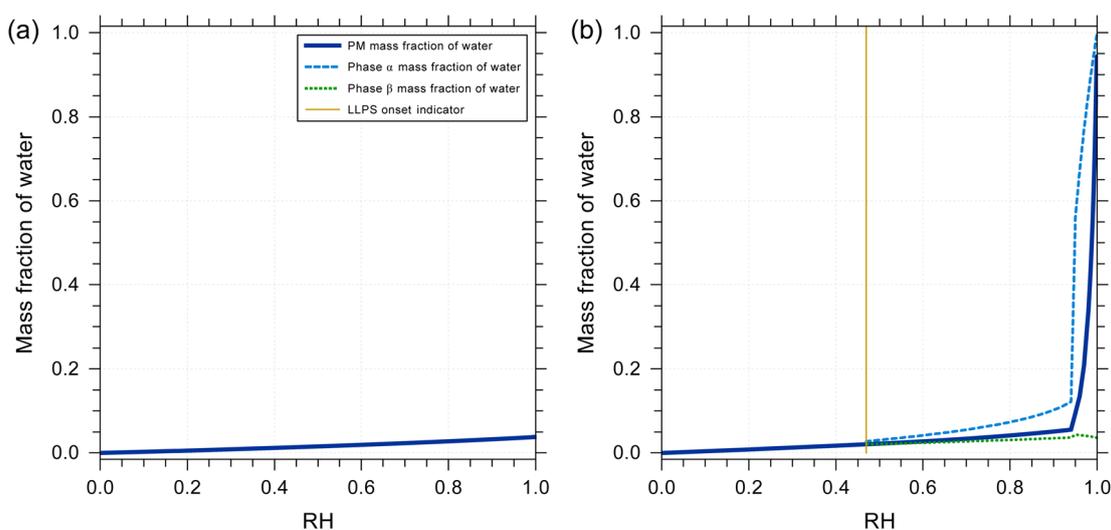

Fig. 1 Predicted equilibrium water uptake of (a) a mixture of squalene ozonolysis products and (b) a mixture of squalene ozonolysis products, levulinic acid and palmitic acid (see mixture composition listed in Table S4†). All predictions were made with the AIOMFAC−LLE model for $T =$ 298 K and variable RH, assuming the dry mixture composition to remain unchanged (nonvolatile) while water uptake and LLPS were considered. (b) The system containing levulinic and palmitic acids exhibits LLPS for RH > 0.47.

52 | Environ. Sci.: Atmos., 2023, 3, 49–64

© 2023 The Author(s). Published by the Royal Society of Chemistry

products would partition from the well-mixed film to the flow tube gas phase irreversibly, which is consistent with the small thicknesses of the films of approximately 12–39 nm (see Table S3†), compared to the volume of the flow tube (>1 L) and the short gas molecule residence time in the flow tube (~40 seconds). Several changes which are specific to the skin oil model are made. Squalene is assumed to account for ~10% of the skin oil and an additional initial carboxylic acid concentration, which accounts for ~25% of the skin oil is also included.[1] Of the initial carboxylic acids, 25% are assumed to be palmitic acid.[1] An additional reaction to treat these carboxylic acids already present in the skin with CIs is included and is shown as reaction 539 (skin oil acids + all Criegee intermediates → products) in Table S1.† For the skin oil model, the volume of the oil is fixed and does not change over time. The thickness is uncertain and set to 39 nm based on the assumption that a typical fingerprint (consisting of deposited skin oils) weighs 10 μg and has a surface area of 3 cm^2.[60,61] The partitioning coefficient of water into the skin oil is also set to a fixed value, as this process is likely controlled by hydrophilic species present in the skin oil such as glycerols and acids and was determined by fitting to experimental data.[1]

Modeling the ozonolysis products from soiled T-shirts and people

The clothing and KM-SUB-Skin-Clothing models have previously been described in detail and, therefore, only a brief description will follow here.[33] KM-SUB-Skin-Clothing consists of many different layers including a gas phase, boundary layer, clothing, gap between the clothing and the skin, surface, skin oils stratum corneum, viable epidermis and underlying blood vessels. Mass transport occurs between and within the layers and many of the layers are split such that diffusion lengths becomes small and the resolution of any concentration gradients within the model increases. Transport of volatile species in the clothing occurs *via* gas-phase diffusion, which is effectively slowed down by a porosity factor and by partitioning into skin oils and other species present on the fibers of the clothing. Contact transfer between the skin oil and the clothing is also included. Note that for the clothing model (in the absence of people and only clothing present in the chamber) the model is reduced to only contain the gas phase, boundary layer and clothing and contact transfer is switched off. Similarly, to the skin oil film model described above, an initial concentration of carboxylic acids is included in the clothing, skin oil and stratum corneum. It is also assumed that an initial concentration of other species containing double bonds is initially present, which is treated using reactions 540–545 in Table S1.† The clothing model is applied to squalene ozonolysis measurements made when 4 soiled T-shirts were exposed to ozone during the Indoor Chemical Human Emissions and Reactivity (ICHEAR) project,[24,62] while the KM-SUB-Skin-Clothing model is applied to measurements of two people entering a chamber which contained ozone.[5] More information regarding the experimental methods can be found in these publications.[5,24,62]

Determination of parameters to reproduce the experimental data

Parameter values used in the models are summarized in Table S3† with explanations regarding the determination of their values. The experimental measurements were fitted by applying a combination of the Monte Carlo Genetic Algorithm (MCGA) and a simplex algorithm to obtain uncertain parameters.[63] Uncertain parameters included the rate coefficients in the gas and condensed bulk phases, the partitioning coefficients of ozone, water, and the volatile products, the boundary layer thickness next to the clothing and the concentration of other reactive species within the clothing. During the Monte Carlo stage of the optimization process, these parameters were each varied over a range of values, which incorporated any published values. A fitness value to the data was assigned to each parameter set. During the genetic algorithm stage, the best model parameter sets were improved using processes which occur naturally during evolution such as combination, survival, and mutation. The best parameter set was then further improved using the simplex optimization method which was run several times until a parameter set which did not contain any unrealistic values was obtained.

Although most parameters were consistent between scenarios, it was necessary to slightly change the values of some parameters between different scenarios (Table S3†). This most likely reflects model simplifications such as missing processes or reactions and uncertainties in some of the measurements. Missing processes may impact the modeled scenarios in different ways due to the different conditions of the experiments leading to the apparent changes in the rate coefficients. Examples of processes that could be included in the model in the future, but are complex and not currently fully understood, are reversible and non-reversible losses of species at the chamber or flow tube surfaces. There are several factors that could influence these losses including the surface-to-volume ratio, the composition and reactivity of the surface, the porosity of the surface and the flow conditions. By not including wall losses in the model, the reported product formation rates are effectively lowered to compensate for the additional loss term. The extent of this effect is different in each model scenario. It should also be noted that the MCGA does not consider potential measurement errors arising from uncertainties in the product absorption cross-sections and ion fragmentation. Our study is a first attempt at modeling and better understanding the complex processes controlling gas-phase concentrations of squalene ozonolysis products as a function of relative humidity. All rate coefficients were within two orders of magnitude among different scenarios with most being much closer or identical making them relatively consistent. Additional processes and reactions could be added in the future as they become better understood, which would ideally make parameters fully consistent among different scenarios.

Initially the MCGA was applied to the squalene particle experiments and parameters were obtained. Sensitivity tests indicated the parameters that could lead to the biggest improvement in the fitting, and these were further optimized

© 2023 The Author(s). Published by the Royal Society of Chemistry

Environ. Sci.: Atmos., 2023, **3**, 49–64 | **53**

using the simplex algorithm. The MCGA and simplex algorithms were subsequently run for the other scenarios, while keeping consistency with the parameters determined for the squalene particle modeling. For these runs only parameters that had not been determined were allowed to vary (*e.g.*, for the ICHEAR data this included the boundary layer length, the partitioning coefficients for clothing and initial concentrations in clothing). Sensitivity tests were then performed to determine additional parameters that could lead to the biggest improvements in the fitting and would need to be varied to fit measurements. The MCGA and simplex algorithms were subsequently rerun leading to differences in some parameters

between the different scenarios. This process was then repeated to try and minimize the differences in parameters for the different scenarios.

Results and discussion

Pure squalene particles

Fig. 2 shows the decay of squalene (panel a), the decrease in particle radius (panel b), the formation of bulk-phase products (panels c and d) and the formation of gas-phase products (panels e–l) when pure squalene particles were exposed to different ozone concentrations and different RHs as measured
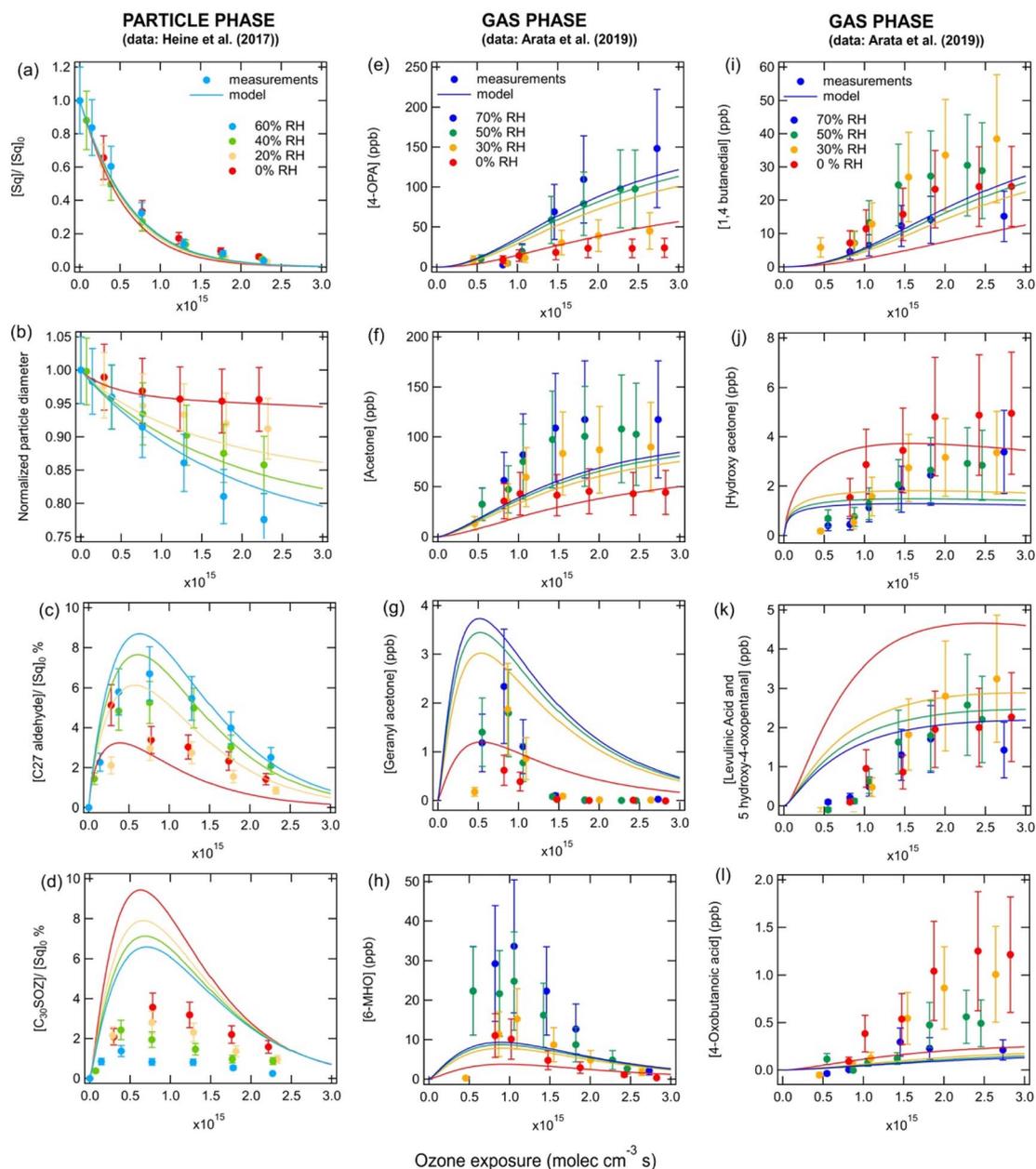

Fig. 2 Measurements (markers) and model outputs (lines) of the (a) decay of squalene, (b) decrease in particle diameter, (c and d) bulk phase products and (e–l) gas-phase products as a function of ozone exposure and RH for 300 nm pure squalene particles at room temperature. Measurements are from (a–d) Heine *et al.*[23] and (e–l) Arata *et al.*[24]

54 | *Environ. Sci.: Atmos.*, 2023, **3**, 49–64

© 2023 The Author(s). Published by the Royal Society of Chemistry

by Heine et al.[23] and Arata et al.[24] The model captures most of the experimentally observed trends, but some of the absolute concentrations were not within a factor of two of the measurements. As previously discussed by Heine et al.,[23] the decay of squalene as a function of ozone exposure, shown in Fig. 2a, is independent of relative humidity, as it is controlled solely by reaction (R1). The decrease in particle size under high ozone exposures and high RHs, shown in Fig. 2b, is due to the formation of more (semi)volatile secondary carbonyls which partition to the gas phase. Fig. 2c and d show the concentrations of a C27 carbonyl product and a C30 secondary ozonide product in the particles, respectively. As the ozone exposure increases, these products are formed, but further increases in ozone concentrations lead to their destruction as they both contain many double bonds. The normalized carbonyl product concentration increases with RH due to the direct reaction of CIs with water (reaction (R2)), while the secondary ozonide product decreases due to the competitive nature of reactions (R2) and (R5). It should be noted that, similarly to the model in Heine et al.,[23] our model predicts higher C30 secondary ozonide concentrations than were measured, which may be due to simplifications in the model, an incomplete mechanism or uncertainties in the absolute measured product abundance

which arises from uncertainties in the product absorption cross-sections and ion fragmentation.[23] There are no standards for secondary ozonides and therefore no direct calibrations can be performed. This may also affect all scenarios in this work where data was derived by PTR-MS. These factors may also account for discrepancies between the measurements and modeled normalized concentrations (curves in Fig. 2) for some of the gas phase species.

The model results and most experimental measurements suggest that carbonyl species in the gas phase (Fig. 2, panels e–i) increase with increasing RH due to the reaction of CIs with water (reaction (R2)). Two of the carbonyl species contain double bonds (geranyl acetone and 6-MHO); thus, these species are destroyed as ozone exposures become high, while the three other carbonyl products which contain no double bonds (acetone, 4-OPA and 1,4-butanedial) continue to increase. Gas-phase carboxylic acids and hydroxy ketones (panels j–l) are formed via the self-rearrangement of the CI (reaction (R4)). Therefore, higher concentrations are predicted by the model at low RH, as the competition from the CI + H_2O (reaction (R5)) pathway decreases. As ozone concentrations increase, the model predicts that the concentrations of the carboxylic acids and hydroxy ketones increase, as more CIs are formed, but then
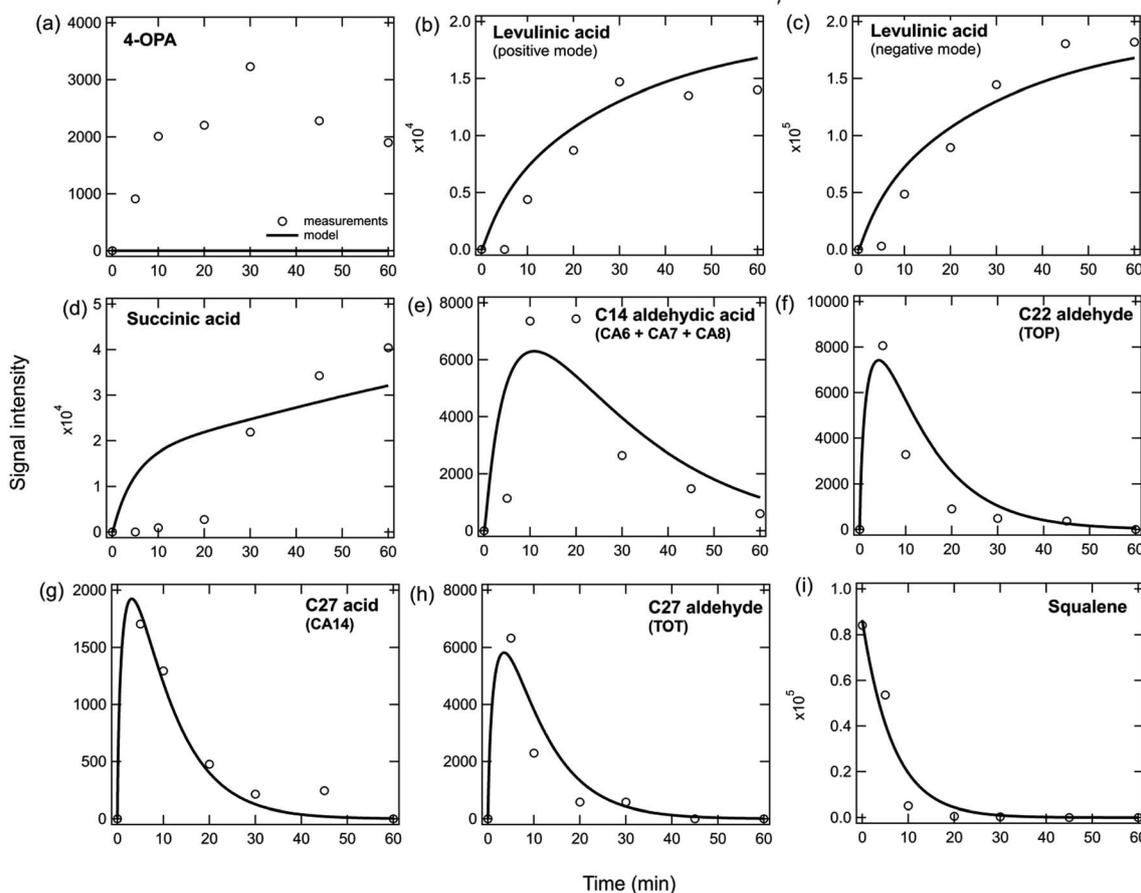

Fig. 3 Measurements (markers) and model outputs (lines) of the temporal evolution of bulk squalene and products when a pure squalene film is exposed to 50 ppb of ozone at room temperature. Scaling factors were used to match the modeled data to the measured signal intensity which was not calibrated. Measurements are from Zhou et al.[2]

© 2023 The Author(s). Published by the Royal Society of Chemistry

Environ. Sci.: Atmos., 2023, **3**, 49–64 | 55

start to plateau as the competitive reaction (R3) becomes important. The model can also be used to estimate the concentrations of species in the particles grouped by functionalities (Fig. S1†). Secondary ozonides are predicted to be the most abundant condensed-phase product under most scenarios followed by carbonyls. Bulk concentrations of carboxylic acids, hydroperoxides and hydroxy ketones are likely more than two orders of magnitude lower than secondary ozonides. As RH increases, bulk carbonyl concentrations increase, while the concentration of all other species decrease. Note that the concentrations of species such as secondary ozonides and hydroperoxides, shown in Fig. S1,† must be regarded as upper limits, as their decomposition is not included in the model due to a lack of data regarding the rate at which this occurs. It should also be noted that one previous study has estimated the bulk phase composition of squalene ozonolysis products and predicted that 42.5% of oxygen atoms should be present in peroxy groups.[3]

Squalene and skin oil films

Fig. 3 shows the signal intensity of many condensed bulk phase products measured by Zhou *et al.*[2] using direct analysis in real time mass spectrometry (DART-MS) when a pure squalene film was exposed to ozone under dry conditions. The model can

reproduce the temporal evolution of different products relatively well with similar rate coefficients to those used in the pure squalene particle model (Table S3†). The results show that the increase over time of terminal products (levulinic acid and succinic acid, Fig. 3b–d) and the decrease of squalene (Fig. 3i) is well reproduced by the model. The increase and subsequent decrease of products containing double bonds can also be reproduced (Fig. 3e–h). It should be noted that 4-OPA is volatile and would be unlikely to remain in the bulk under the conditions of the experiment unless there are processes occurring that are currently not well understood and untreated in the model (Fig. 3a). It may also be possible that the 4-OPA signal represents a different compound (*e.g.*, a less volatile acid). Levulinic acid and succinic acid are semi-volatile, but they were forced to remain in the condensed phase and not allowed to partition into the gas phase in the model in order to reproduce their measurements, which could also indicate that there may be a missing chemical or physical process in the model. For example, we speculate that the presence of even a small amount of water could lead to the formation of the levulinate and succinate conjugate bases. These species could also absorb to glass which may preferentially keep them on the surface. However, due to uncertainty regarding whether a sufficient amount of water was present in the system and the binding
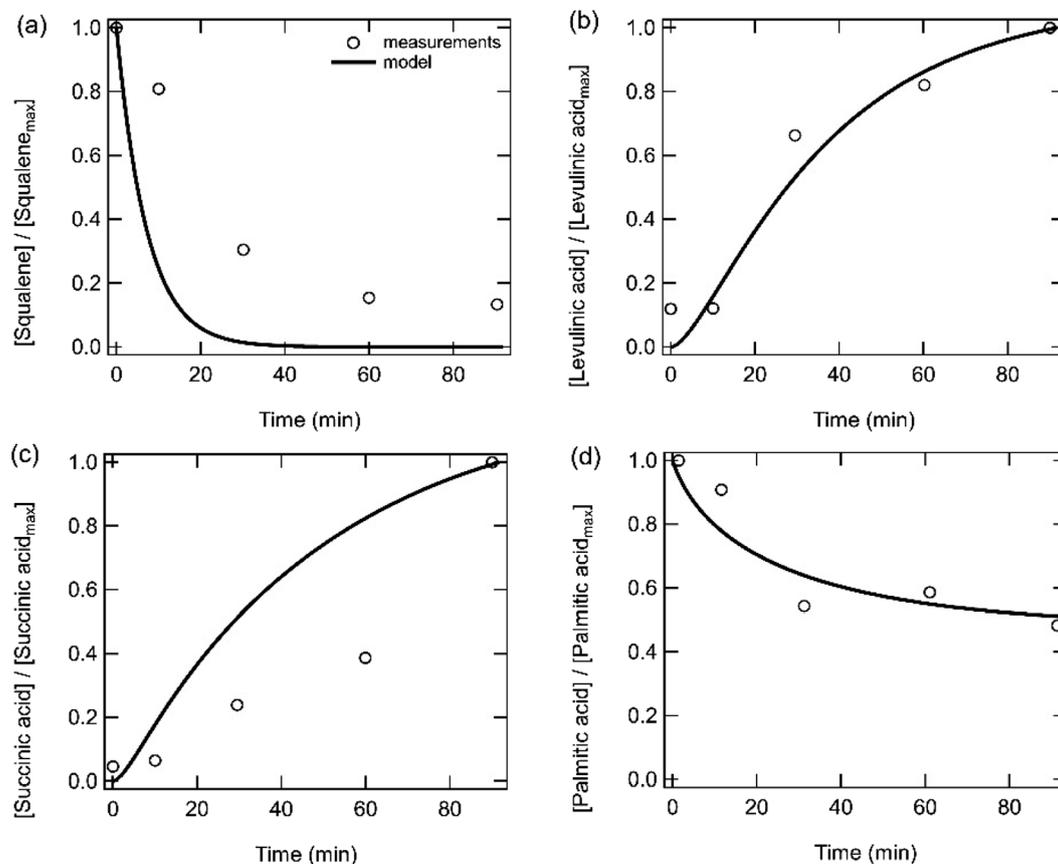

Fig. 4 Measurements (markers) and model outputs (lines) of the temporal evolution of bulk (a) squalene, (b) levulinic acid, (c) succinic acid and (d) palmitic acid when a skin oil film is exposed to 50 ppb ozone at room temperature. Measurements and model outputs have been normalized to the maximum signal or concentration. Measurements are from Zhou *et al.*[4]

strengths of these acids to glass, we have not tried to model these processes explicitly. Concentrations of species grouped by functionalities and as a function of time in the condensed phase have been calculated (Fig. S2a†) and are in good agreement with the pure squalene particle results (Fig. S1†).

Fig. 4 shows the time evolution of bulk phase squalene, levulinic acid, succinic acid, and palmitic acid when skin oil is exposed to ozone under dry conditions as measured by Zhou *et al.*[4] The measured squalene decay is significantly slower in the skin oil (Fig. 4a) than in the pure squalene film (Fig. 3i). The same rate coefficient for double bonds with ozone and a similar small film thickness (12–39 nm, resulting in ozone saturating the film) are used in the models for both systems (Table S3†), resulting in an overprediction of the squalene decay in the skin oil. Sensitivity calculations also indicated that the film thickness could be changed by two orders of magnitude without substantially impacting the model outputs. The measured slow squalene decay has previously been attributed to a squalene burial within the skin oil bulk which would lead to less squalene exposure to ozone at the surface.[4] We expect that this burial mechanism could happen for various reasons such as a change in film or surface viscosity due to phase separation and crust formation as products form.[64,65] The formation of a new semi-solid or solid phase has recently been observed for squalene and skin oil proxy particles that have been exposed to high concentrations of ozone.[66] However, due to uncertainties in the exact mechanism that causes the slower squalene decay, such potential surface crust formation and associated kinetic limitations are not treated in the model. We can also speculate that such a burial process may be affected by temperature and may be different on room surfaces compared to human skin. Levulinic acid and succinic acid are relatively well reproduced by the model (note that these were treated as non-volatile, which may indicate that they are binding to glass surfaces in the experimental setup or with bases such as amines which may be present in skin oil[67] or that there may be a small amount of water present in the system leading to the formation of the levulinate and succinate conjugate bases) (Fig. 4b and c). Skin-surface pH is reported to be in the range of 4.1–5.8 with a mean of 4.9.[68] The pK_a values of levulinic and succinic acids are below the mean (4.6 and 4.2)[69,70] pH suggesting that, if enough water is present, then much or most of these acids can be present in their non-volatile, conjugate base form. Palmitic acid, which is present in skin oil and contains no double bonds, is observed to decay over time, which can be reproduced with the model by adjusting the rate coefficient of reaction (R6) that treats the reaction of CIs with carboxylic acids. Concentrations of species grouped by functionalities and as a function of time in the skin oil film have been calculated (Fig. S2b†). The total bulk product concentration in skin oil (Fig. S2b†) is lower than that for the pure squalene film (Fig. S2a†) due to the lower initial squalene concentration in the film. Hydroperoxide concentrations are relatively higher in the skin oil film compared to the squalene film due to the reaction of carboxylic acids present in skin oil with CIs.

For comparison with the pure squalene system and in to order to investigate the potential for phase separation in skin oil, the AIOMFAC model was used to predict the water uptake of a system consisting of the surrogate compounds listed in Table S4† plus palmitic acid and levulinic acid (here of a molar ratio of 1 : 1 : 1 for surrogate mixture : palmitic acid : levulinic acid). The predicted mass fraction of water as a function of RH is shown in Fig. 1b. In this case, the more polar and hygroscopic organic acids contribute substantially to the water uptake at higher RH. Their presence also leads to LLPS for RH > 47%, see Fig. S3b.† The water-rich phase is particularly distinct in composition for RH > 95%, where levulinic acid and water dominate that phase, while a wider selection of squalene oxidation products contributes to that phase for RH < 95% (Fig. S3b†). These equilibrium partitioning predictions suggest that a fraction of the squalene oxidation products will partition into a more polar, water-containing phase when present in/on the skin. However, the AIOMFAC–LLE predictions of the phase compositions under LLPS conditions also indicate that for RH < 95%, the mixture of organic compounds, including the organic acids, remains diverse in composition in both phases. LLPS is not currently treated in the kinetic model and there are also many other species present in skin oil, such as glycerol and pyroglutamic acid which are both humectants, that should be included in AIOMFAC simulations in the future.[1,4] For these reasons the gas-to-skin oil water partitioning coefficient in the kinetic model was set to a fixed value and determined by fitting to experimental measurements. However, in the future added complexity should be added to both the AIOMFAC simulations and the treatment of partitioning in the kinetic model.

ICHEAR data and KM-SUB-Skin-Clothing

Fig. 5 shows measurements and modeling of the temporal evolution of gas-phase species when 4 soiled T-shirts were exposed to ozone during the ICHEAR campaign[24,62] for both variable and fixed RHs. The effect of the changing RH can clearly be seen in the measurements and model outputs for acetone and 6-MHO (Fig. 5e and g), with higher RHs leading to more of these carbonyl species forming due to reaction (R2). The model predicts that hydroxyacetone will decrease with increasing RH, since it is formed by reaction (R4), which directly competes with the reaction of CIs with water (Fig. 5i). However, the opposite trend is observed in the measurements, indicating that there may be other RH-dependent physical processes such as RH-dependent partitioning to room surfaces and competitive adsorption of water and squalene ozonolysis products.[71–75] Hydroxyacetone is polar and water soluble, so we may expect more partitioning to surfaces covered in aqueous films under high RH conditions. However, this would increase hydroxyacetone surface concentrations and reduce gas-phase concentrations upon an increase of RH. The measurements show the opposite trend, suggesting that this is not the dominant process that occurs. We can also speculate that the partition coefficient of hydroxyacetone precursors may change for surface films containing different concentrations of water, leading to hydroxyacetone being formed at different overall rates and increasing its gas-phase concentration at higher RH. Future studies should investigate whether hydroxyacetone can be

© 2023 The Author(s). Published by the Royal Society of Chemistry
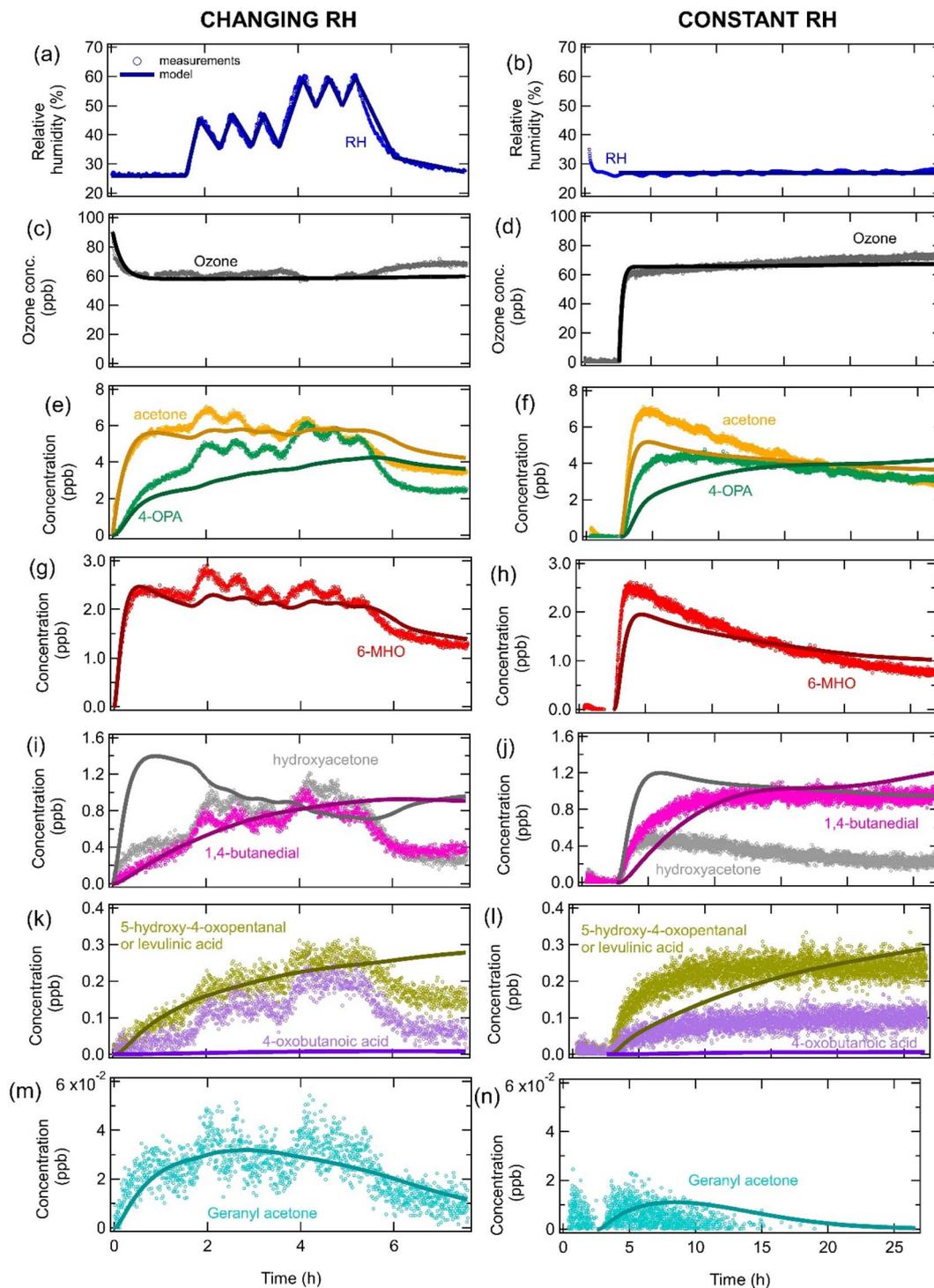
Environ. Sci.: Atmos., 2023, **3**, 49–64 | 57

Fig. 5 Measurements (markers) and model outputs (lines) of the temporal evolution of (a and b) RH, (c and d) ozone, and (e–n) gas-phase squalene ozonolysis products after four soiled T-shirts are exposed to ozone under (left hand side panels) changing RH conditions and (right hand side panels) constant RH as part of the ICHEAR experiments. All measurements have had the background concentrations subtracted for simplicity when modeling. Measurements for the changing RH conditions are from Arata et al.[24] and were performed at a temperature of 27.4–28.3 °C. The data at a constant RH is from ICHEAR experiments performed on the 19–20 May 2019.

displaced by water molecules on surfaces leading to it having lower surface concentrations and higher gas-phase concentrations at higher relative RH on different indoor relevant. Although this has not yet been investigated experimentally or

theoretically for hydroxyacetone, measurements have shown that limonene can be displaced by water from hydroxylated SiO_2, which is a surrogate for glass surfaces.[75] There may also be missing reaction pathways in the model or another compound

may be emitted from the clothing which contributes to the hydroxyacetone signal. We have not tried to explicitly test any of these hypotheses in the model due to too many uncertainties being associated with them. Further studies are required to identify important processes and to determine parameters that could be used in the model. Similarly to hydroxyacetone, the measurements show that 4-oxobutanoic acid, 5-hydroxy-4-oxopentanal and levulinic acid decreased with decreasing RH, which is the opposite of the expected trend based on the chemical mechanism (Fig. 5k) and may be due to some of the factors discussed above. The model predicts that 5-hydroxy-4-oxopentanal dominates the signal in Fig. 5k. The model shows a dampened response to RH for 4-OPA, 5-hydroxy-4-oxopentanal and 1,4-butanedial, as these species form slowly and continuously over time from a variety of precursors and accumulate in the gas phase. Similarly, the impact of RH is not observed for geranyl acetone, which initially increases as it forms and accumulates, but then decreases due to a decrease in the concentration of its precursors (*e.g.*, squalene) in the clothing. 4-Oxobutanoic acid is significantly underestimated by the model, which was also observed in Fig. 2, indicating that the mechanism may be incomplete. When reproducing the fixed RH data, slightly different parameters linked to the soiling level of the clothing were used in the model compared to when modeling the changing RH data. For the fixed RH scenario, gas-phase concentrations of many compounds decrease over time due to the decreasing squalene concentration in the clothing over time.

It should be noted that although all the rate coefficients used to reproduce the ICHEAR data (parameter sets 3 and 4 in Table S3†) were within one order of magnitude to those used in Fig. 2–4 (parameter sets 1 & 2), they had to be slightly adjusted to optimize the fit. Fig. S4† shows the fitting obtained if the rate coefficients used in Fig. 2 (parameter set 1) are used to model the ICHEAR data. The higher rate coefficient for the conversion of CIs to carboxylic acids and hydroxy ketones ($k_{br,4}$) for parameter set 1 causes carboxylic acids and hydroxy ketones to be significantly overestimated. A similar overestimation was seen for the lower O_3 exposures in Fig. 2(j–k). The lower rate coefficient of CIs reacting with carbonyls ($k_{br,5}$) for parameter set 1 leads to many species containing carbonyl groups being overestimated (*e.g.*, 1,4 butanedial and 5-hydroxy-4-oxopentanal in Fig. S4†). Additionally, the higher rate coefficient of double bonds reacting with O_3 in the gas phase ($k_{1,gas}$) causes gas-phase species containing double bonds to be rapidly destroyed and therefore underestimated by the model (*e.g.* 6-MHO and geranyl acetone in Fig. S4†). The slightly different rate coefficients for the different scenarios may indicate that the reaction mechanism is incomplete, that there are missing processes in the model or uncertainties in the measurements as previously discussed.

The KM-SUB-Skin-Clothing model was also applied to measurements of the temporal evolution of ozone and squalene ozonolysis products when two people entered a chamber at a constant RH (Fig. S5†). The model was able to reproduce the measurements relatively well using parameters which were similar to those used for the ICHEAR measurements (Table S3†

and further discussion below). The partitioning coefficient of geranyl acetone had to be reduced by a factor of four in order to reproduce the relatively larger geranyl acetone gas phase concentrations, while $k_{5,bulk}$ also had to be reduced by a factor of about 70 in order to not underestimate the concentrations of the gas-phase carbonyl products (Fig. S6†). These differences in parameters may indicate missing processes in the model and may also be related to calibration issues with instrumentation as discussed earlier. It should also be noted that people emit many compounds in their breath, such as acetone and isoprene, which has not been treated in the model. Hydroxyacetone may form from the OH initiated oxidation of isoprene which should be considered in future models. It is currently unclear how the OH radical concentrations will vary as a function of RH and this should be investigated in future work.

Extrapolation to different scenarios

Fig. 6 shows sensitivity tests that were performed to better understand the impact that RH could have over a prolonged period on gas-phase squalene ozonolysis products. For these sensitivity tests, the RH was fixed and the conditions of the ICHEAR experiments (parameters used for changing RH in Fig. 5) and the KM-SUB-Skin-Clothing model (parameters used for Fig. S5†) were used with gas-phase concentrations being calculated after four hours. For both scenarios, ozone concentrations remained relatively stable as a function of RH (Fig. S7a†). Ozone loss was dominated by deposition to clothing, although the percentage lost in the gas phase compared to the skin or clothing increased slightly as RH increased and more compounds containing double bonds were emitted to the gas phase (Fig. S7b†). As expected, based on the chemical mechanism, the model predicts that as RH increases gas-phase carbonyl species will increase, while carboxylic acids and hydroxy ketones decrease. The impact for many species is large, for example, for both scenarios 6-MHO concentrations approximately double when RHs increase from 10% RH to 95% RH, which is a typical range of RHs indoors (Fig. 6c).[76,77] This is due to the branching ratios in the model and 6-MHO being a secondary carbonyl; for every 0.1 molecules of 6-MHO that form in the bulk condensed phase, 0.9 molecules of CI2 will form (Table S3†). CI2 can subsequently react with water forming 6-MHO, which accumulates in the gas phase and leads to the large RH dependence. Increasing the RH also causes a large decrease in the hydroxy ketone product (6-methyl-5-ene-2-oxo-heptanol) that can form from CI2 *via* reaction (R3) (Fig. 6e). An increase in the concentration of a species such as 6-MHO, will also lead to an increase in their ozonolysis products, which enhances the impact of RH. Although most species behave in the same way for both scenarios, 4-MOD and 1,4-butanedial increase with increasing RH in the clothing model simulation, but remain almost constant in the KM-SUB-Skin-Clothing model simulation (Fig. 6f and g). The difference in behavior for 4-MOD can be attributed to the different values used for the reaction of carbonyls with CIs ($k_{5,bulk}$) for the two models. At low RHs there are more CIs in the bulk which can react with less volatile carbonyls (*e.g.*, 4-MOD), leading to their destruction if
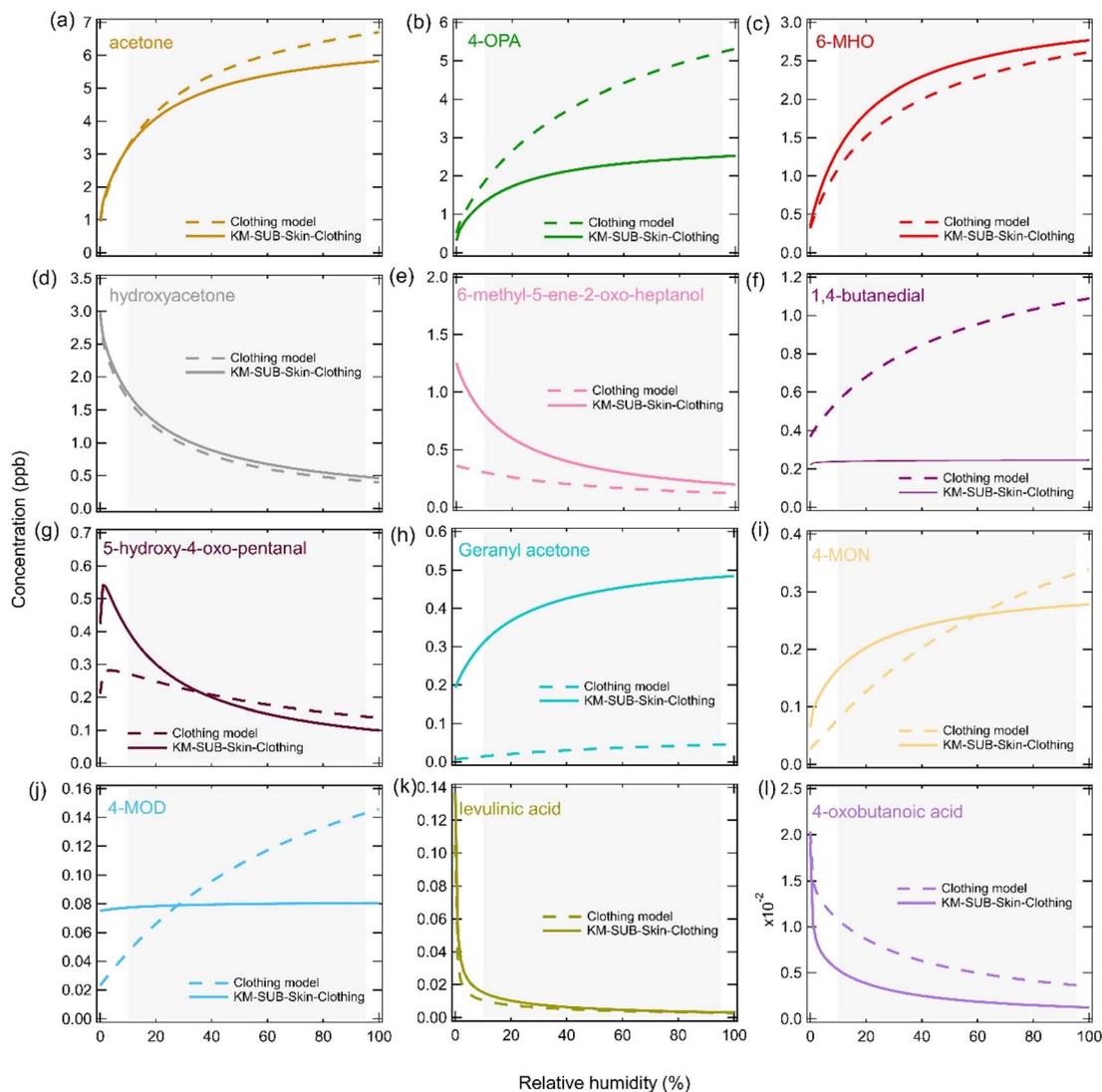
© 2023 The Author(s). Published by the Royal Society of Chemistry

Environ. Sci.: Atmos., 2023, **3**, 49–64 | **59**

Fig. 6 The impact of prolonged RH on the gas-phase concentrations of squalene ozonolysis products. Gas-phase concentrations were calculated after four hours at a fixed RH using the conditions and parameters used in the clothing model to fit the ICHEAR data shown in the left-hand side panels of Fig. 5 (dashed lines) and the conditions and parameters used in the KM-SUB-Skin-Clothing model to fit the data in Fig. S5† (solid lines). The grey shaded area represents typical indoor RHs.

the rate coefficient is elevated enough, such as for the clothing model. 1,4-Butanedial is formed from the ozonolysis of condensed phase species (such as 4-MOD) before it rapidly partitions to the gas phase and therefore has the same RH trend. A test to check the impact of switching off reaction (R6) was also performed, but this had a negligible impact on the gas-phase concentrations shown in Fig. 6.

Conclusions and implications

In this study we developed a chemical mechanism for squalene ozonolysis and implemented it into several models to improve our mechanistic understanding of the formation of products under different RHs. We treat the reaction of ozone with double bonds and the subsequent reaction of CIs. Rate coefficients of different reactions have been constrained to small ranges (Table S3†). In general, we showed that increasing the RH would

increase the concentrations of secondary carbonyls due to the reaction of CIs with water, while species formed from competing pathways, such as carboxylic acids and hydroxy ketones, would decrease. Our previously developed KM-SUB-Skin-Clothing model, which originally only treated carbonyls, now includes additional volatile and semi-volatile products such as carboxylic acids and hydroxy ketones and treats RH effects enabling it to be applied to a wider variety of laboratory chamber studies in the future. We were also able to model the decrease in carboxylic acid concentrations present in skin oil due to their reaction with CIs. However, some processes and chemical reactions may mimic each other, leading to the same modeled gas-phase concentrations and it may not be possible without direct measurements of intermediates to validate the model completely or identify other influential mechanisms.

Although small yet rapid changes in RH may only have a small impact on concentrations of different gas-phase

60 | *Environ. Sci.: Atmos.*, 2023, **3**, 49–64

© 2023 The Author(s). Published by the Royal Society of Chemistry

squalene ozonolysis products, a prolonged change in RH can significantly alter human exposure to carbonyls, carboxylic acids, and hydroxy ketones. Concentrations of many species may change by a factor of two between 10% RH and 95% RH which is a typical RH range indoors. Squalene ozonolysis products are known to have adverse health effects;[12,18–22] it is therefore important to have a tool which allows for their concentrations to be predicted under different indoor conditions. A predictive model can also help in the design and evaluation of personal care products that are intended to protect skin from the adverse effects of air pollution. In addition, it should be noted that many products are likely to be enhanced in the breathing zone as products emitted by skin are transported upwards by a thermal plume around the human body.[35,78] However, chemistry is likely not the only source of a RH dependence of squalene ozonolysis products and RH dependent partitioning to surfaces or diffusion within room surfaces as well as competitive adsorption should be studied in a controlled manner in the future before being implemented as additional processes into models.[71–74] It will also be important in the future to simultaneously treat ozone reactions with occupants within indoor environments as well as ozone reactions of skin oils and flakes that have been deposited to other indoor surfaces and can account for a large fraction of the ozone reactivity in real indoor environments.[36,79] Furthermore, a recent study has shown that elevated OH concentrations may form from the ozonolysis of compounds emitted by people.[80] The consequence of these reactions and any potential relative humidity dependence should be investigated by further developing models.

There remain uncertainties in the model with regards to parameters, the chemical mechanism and processes that should be included in the future. The role of the surface in the overall reaction mechanism should be further investigated and implemented in a future version of the model. Bulk diffusivities of skin lipids and reaction products would need to be treated as a function of RH. Another source of uncertainty is the partitioning of water into squalene, into squalene ozonolysis products and into skin oil. To address this issue the AIOMFAC-based equilibrium model was conducted and predicted a negligible water uptake for pure squalene particles which increased as products formed and was in reasonable agreement with the modeling parameters used in this work. AIOMFAC simulations also predicted that the addition of acids to the mixture, such as present in skin oil, could cause LLPS and lead to the formation of surface crusts that can limit partitioning and multiphase reaction kinetics.[81,82] Further experimental validations as well as simulations with more realistic skin oil compositions including other unsaturated fatty acids and triglycerides[83] are required to further improve our understanding on skin ozonolysis and its impacts on indoor air quality.

Author contributions

P. S. J. L. and M. S. designed the research and developed the kinetic model. P. S. J. L. performed the kinetic modeling simulations. A. Z performed the AIOMFAC modeling. Ja. W. developed an automatic differential equation writer and T. B. developed the Monte Carlo Genetic Algorithm (MCGA) method. C. A, A. H. G, K. R. W, N. W, Jo. W, J. P. D. A conducted and provided experimental measurement data. P. S. J. L and M. S wrote the original draft and all authors reviewed and edited the manuscript.

Conflicts of interest

There are no conflicts to declare.

Acknowledgements

References

1 N. Nicolaides, Skin Lipids – Their Biochemical Uniqueness, *Science*, 1974, **186**, 19–26.

2 S. Zhou, M. W. Forbes and J. P. D. Abbatt, Kinetics and products from heterogeneous oxidation of squalene with ozone, *Environ. Sci. Technol.*, 2016, **50**, 11688–11697.

3 D. R. Fooshee, P. K. Aiona, A. Laskin, J. Laskin, S. A. Nizkorodov and P. F. Baldi, Atmospheric oxidation of squalene: molecular study using COBRA modeling and high-resolution mass spectrometry, *Environ. Sci. Technol.*, 2015, **49**, 13304–13313.

4 S. Zhou, M. W. Forbes, Y. Katrib and J. P. Abbatt, Rapid oxidation of skin oil by ozone, *Environ. Sci. Technol. Lett.*, 2016, **3**, 170–174.

5 A. Wisthaler and C. J. Weschler, Reactions of ozone with human skin lipids: Sources of carbonyls, dicarbonyls, and hydroxycarbonyls in indoor air, *Proc. Natl. Acad. Sci. U. S. A.*, 2010, **107**, 6568–6575.

6 B. Coffaro and C. P. Weisel, Reactions and Products of Squalene and Ozone: A Review, *Environ. Sci. Technol.*, 2022, **56**, 7396–7411.

7 A. Rai, B. Guo, C. H. Lin, J. Zhang, J. Pei and Q. Chen, Ozone reaction with clothing and its initiated VOC emissions in an environmental chamber, *Indoor Air*, 2014, **24**, 49–58.

8 B. K. Coleman, H. Destaillats, A. T. Hodgson and W. W. Nazaroff, Ozone consumption and volatile byproduct formation from surface reactions with aircraft cabin materials and clothing fabrics, *Atmos. Environ.*, 2008, **42**, 642–654.

9 A. Wisthaler, G. Tamás, D. P. Wyon, P. Strøm-Tejsen, D. Space, J. Beauchamp, A. Hansel, T. D. Märk and C. J. Weschler, Products of ozone-initiated chemistry in a simulated aircraft environment, *Environ. Sci. Technol.*, 2005, **39**, 4823–4832.

© 2023 The Author(s). Published by the Royal Society of Chemistry

Environ. Sci.: Atmos., 2023, **3**, 49–64 | 61

10 X. Tang, P. K. Misztal, W. W. Nazaroff and A. H. Goldstein, Volatile organic compound emissions from humans indoors, *Environ. Sci. Technol.*, 2016, **50**, 12686–12694.

11 S. Liu, R. Li, R. Wild, C. Warneke, J. de Gouw, S. Brown, S. Miller, J. Luongo, J. Jimenez and P. Ziemann, Contribution of human-related sources to indoor volatile organic compounds in a university classroom, *Indoor Air*, 2016, **26**, 925–938.

12 S. E. Anderson, J. Franko, L. G. Jackson, J. Wells, J. E. Ham and B. Meade, Irritancy and allergic responses induced by exposure to the indoor air chemical 4-oxopentanal, *Toxicol. Sci.*, 2012, **127**, 371–381.

13 S. E. Anderson, J. Wells, A. Fedorowicz, L. F. Butterworth, B. Meade and A. E. Munson, Evaluation of the contact and respiratory sensitization potential of volatile organic compounds generated by simulated indoor air chemistry, *Toxicol. Sci.*, 2007, **97**, 355–363.

14 J. Jarvis, M. Seed, R. Elton, L. Sawyer and R. Agius, Relationship between chemical structure and the occupational asthma hazard of low molecular weight organic compounds, *Occup. Environ. Med.*, 2005, **62**, 243–250.

15 J. J. Thiele, M. Podda and L. Packer, Tropospheric ozone: an emerging environmental stress to skin, *Biol. Chem.*, 1997, **378**, 1299–1306.

16 D. Lipsa, J. Barrero-Moreno and M. Coelhan, Exposure to selected limonene oxidation products: 4-OPA, IPOH, 4-AMCH induces oxidative stress and inflammation in human lung epithelial cell lines, *Chemosphere*, 2018, **191**, 937–945.

17 P. Wolkoff, S. T. Larsen, M. Hammer, V. Kofoed-Sørensen, P. A. Clausen and G. D. Nielsen, Human reference values for acute airway effects of five common ozone-initiated terpene reaction products in indoor air, *Toxicol. Lett.*, 2013, **216**, 54–64.

18 R. Kreiling, H. M. Hollnagel, L. Hareng, D. Eigler, M. S. Lee, P. Griem, B. Dreeßen, M. Kleber, A. Albrecht and C. Garcia, Comparison of the skin sensitizing potential of unsaturated compounds as assessed by the murine local lymph node assay (LLNA) and the guinea pig maximization test (GPMT), *Food Chem. Toxicol.*, 2008, **46**, 1896–1904.

19 D. M. Pham, B. Boussouira, D. Moyal and Q. Nguyen, Oxidization of squalene, a human skin lipid: a new and reliable marker of environmental pollution studies, *Int. J. Cosmet. Sci.*, 2015, **37**, 357–365.

20 M. J. Roberts, G. T. Wondrak, D. C. Laurean, M. K. Jacobson and E. L. Jacobson, DNA damage by carbonyl stress in human skin cells, *Mutat. Res., Fundam. Mol. Mech. Mutagen.*, 2003, **522**, 45–56.

21 B. Krecisz and M. Kieć-Swierczyńska, The role of formaldehyde in the occurrence of contact allergy (article in Polish), *Med. Pr.*, 1998, **49**, 609–614.

22 J. Patočka and K. Kuča, Irritant Compounds: Aldehydes Review article, *Vojen. Zdrav. Listy*, 2014, **83**, 151–164.

23 N. Heine, F. A. Houle and K. R. Wilson, Connecting the elementary reaction pathways of criegee intermediates to the chemical erosion of squalene interfaces during ozonolysis, *Environ. Sci. Technol.*, 2017, **51**, 13740–13748.

24 C. Arata, N. Heine, N. Wang, P. K. Misztal, P. Wargocki, G. Beko, J. Williams, W. W. Nazaroff, K. R. Wilson and A. H. Goldstein, Heterogeneous Ozonolysis of Squalene: Gas-Phase Products Depend on Water Vapor Concentration, *Environ. Sci. Technol.*, 2019, **53**, 14441–14448.

25 Z. Zhou, P. S. Lakey, M. von Domaros, N. Wise, D. J. Tobias, M. Shiraiwa and J. P. Abbatt, Multiphase Ozonolysis of Oleic Acid-Based Lipids: Quantitation of Major Products and Kinetic Multilayer Modeling, *Environ. Sci. Technol.*, 2022, **56**, 7716–7728.

26 S. Zhou, S. Joudan, M. W. Forbes, Z. Zhou and J. P. Abbatt, Reaction of Condensed-Phase Criegee Intermediates with Carboxylic Acids and Perfluoroalkyl Carboxylic Acids, *Environ. Sci. Technol. Lett.*, 2019, **6**, 243–250.

27 C. J. Weschler and N. Carslaw, Indoor Chemistry, *Environ. Sci. Technol.*, 2018, **52**, 2419–2428.

28 C. Weschler, Chemistry in indoor environments: 20 years of research, *Indoor Air*, 2011, **21**, 205–218.

29 J. P. Abbatt and C. Wang, The atmospheric chemistry of indoor environments, *Environ. Sci.: Processes Impacts*, 2019, **22**, 25–48.

30 T. Salthammer and G. C. Morrison, Temperature and indoor environments, *Indoor Air*, 2022, **32**, e13022.

31 B. C. McDonald, J. A. De Gouw, J. B. Gilman, S. H. Jathar, A. Akherati, C. D. Cappa, J. L. Jimenez, J. Lee-Taylor, P. L. Hayes and S. A. McKeen, Volatile chemical products emerging as largest petrochemical source of urban organic emissions, *Science*, 2018, **359**, 760–764.

32 M. Shiraiwa, N. Carslaw, D. J. Tobias, M. S. Waring, D. Rim, G. Morrison, P. S. Lakey, M. Kruza, M. Von Domaros and B. E. Cummings, Modelling consortium for chemistry of indoor environments (MOCCIE): integrating chemical processes from molecular to room scales, *Environ. Sci.: Processes Impacts*, 2019, **21**, 1240–1254.

33 P. S. J. Lakey, G. C. Morrison, Y. Won, K. M. Parry, M. von Domaros, D. J. Tobias, D. Rim and M. Shiraiwa, The impact of clothing on ozone and squalene ozonolysis products in indoor environments, *Commun. Chem.*, 2019, **2**, 56.

34 P. S. J. Lakey, A. Wisthaler, T. Berkemeier, T. Mikoviny, U. Pöschl and M. Shiraiwa, Chemical kinetics of multiphase reactions between ozone and human skin lipids: implications for indoor air quality and health effects, *Indoor Air*, 2017, **27**, 816–828.

35 Y. Won, P. S. Lakey, G. Morrison, M. Shiraiwa and D. Rim, Spatial Distributions of Ozonolysis Products From Human Surfaces In Ventilated Rooms, *Indoor Air*, 2020, **30**, 1229–1240.

36 M. Zhang, J. Xiong, Y. Liu, P. K. Misztal and A. H. Goldstein, Physical–Chemical Coupling Model for Characterizing the Reaction of Ozone with Squalene in Realistic Indoor Environments, *Environ. Sci. Technol.*, 2021, **55**, 1690–1698.

37 M. Zhang, Y. Gao and J. Xiong, Characterization of the off-body squalene ozonolysis on indoor surfaces, *Chemosphere*, 2022, **291**, 132772.

38 J. Xiong, Z. He, X. Tang, P. K. Misztal and A. H. Goldstein, Modeling the time-dependent concentrations of primary and secondary reaction products of ozone with squalene in a university classroom, *Environ. Sci. Technol.*, 2019, **53**, 8262–8270.

39 M. I. Jacobs, B. Xu, O. Kostko, N. Heine, M. Ahmed and K. R. Wilson, Probing the heterogeneous ozonolysis of squalene nanoparticles by photoemission, *J. Phys. Chem. A*, 2016, **120**, 8645–8656.

40 L. Petrick and Y. Dubowski, Heterogeneous oxidation of squalene film by ozone under various indoor conditions, *Indoor Air*, 2009, **19**, 381–391.

41 L. Lee and K. Wilson, The Reactive–Diffusive Length of OH and Ozone in Model Organic Aerosols, *J. Phys. Chem. A*, 2016, **120**, 6800–6812.

42 T. Berkemeier, A. Mishra, C. Mattei, A. J. Huisman, U. K. Krieger and U. Pöschl, Ozonolysis of Oleic Acid Aerosol Revisited: Multiphase Chemical Kinetics and Reaction Mechanisms, *ACS Earth Space Chem.*, 2021, **5**, 3313–3323.

43 M. Von Domaros, Y. Liu, J. L. Butman, E. Perlt, F. M. Geiger and D. J. Tobias, Molecular Orientation at the Squalene/Air Interface from Sum Frequency Generation Spectroscopy and Atomistic Modeling, *J. Phys. Chem. B*, 2021, **125**, 3932–3941.

44 M. Zeng, N. Heine and K. R. Wilson, Evidence that Criegee intermediates drive autoxidation in unsaturated lipids, *Proc. Natl. Acad. Sci. U. S. A.*, 2020, **117**, 4486–4490.

45 H. Tong, A. M. Arangio, P. S. J. Lakey, T. Berkemeier, F. Liu, C. J. Kampf, W. H. Brune, U. Pöschl and M. Shiraiwa, Hydroxyl radicals from secondary organic aerosol decomposition in water, *Atmos. Chem. Phys.*, 2016, **16**, 1761–1771.

46 C. A. Taatjes, D. E. Shallcross and C. J. Percival, Research frontiers in the chemistry of Criegee intermediates and tropospheric ozonolysis, *Phys. Chem. Chem. Phys.*, 2014, **16**, 1704–1718.

47 M. J. Newland, C. Mouchel-Vallon, R. Valorso, B. Aumont, L. Vereecken, M. E. Jenkin and A. R. Rickard, Estimation of mechanistic parameters in the gas-phase reactions of ozone with alkenes for use in automated mechanism construction, *Atmos. Chem. Phys.*, 2022, **22**, 6167–6195.

48 R. Atkinson and S. M. Aschmann, Hydroxyl radical production from the gas-phase reactions of ozone with a series of alkenes under atmospheric conditions, *Environ. Sci. Technol.*, 1993, **27**, 1357–1363.

49 M. Zeng and K. R. Wilson, Efficient Coupling of Reaction Pathways of Criegee Intermediates and Free Radicals in the Heterogeneous Ozonolysis of Alkenes, *J. Phys. Chem. Lett.*, 2020, **11**, 6580–6585.

50 M. Beck, R. Winterhalter, F. Herrmann and G. Moortgat, The gas-phase ozonolysis of α-humulene, *Phys. Chem. Chem. Phys.*, 2011, **13**, 10970–11001.

51 C. C. Womack, M.-A. Martin-Drumel, G. G. Brown, R. W. Field and M. C. McCarthy, Observation of the simplest Criegee intermediate CH2OO in the gas-phase ozonolysis of ethylene, *Sci. Adv.*, 2015, **1**, e1400105.

52 P. Neeb, O. Horie and G. K. Moortgat, Formation of secondary ozonides in the gas-phase ozonolysis of simple alkenes, *Tetrahedron Lett.*, 1996, **37**, 9297–9300.

53 Q. Ma, X. Lin, C. Yang, B. Long, Y. Gai and W. Zhang, The influences of ammonia on aerosol formation in the ozonolysis of styrene: roles of Criegee intermediate reactions, *R. Soc. Open Sci.*, 2018, **5**, 172171.

54 M. Shiraiwa, C. Pfrang, T. Koop and U. Poeschl, Kinetic multi-layer model of gas-particle interactions in aerosols and clouds (KM-GAP): linking condensation, evaporation and chemical reactions of organics, oxidants and water, *Atmos. Chem. Phys.*, 2012, **12**, 2777–2794.

55 A. Zuend, C. Marcolli, B. P. Luo and T. Peter, A thermodynamic model of mixed organic-inorganic aerosols to predict activity coefficients, *Atmos. Chem. Phys.*, 2008, **8**, 4559–4593.

56 A. Zuend, C. Marcolli, A. Booth, D. Lienhard, V. Soonsin, U. Krieger, D. Topping, G. McFiggans, T. Peter and J. Seinfeld, New and extended parameterization of the thermodynamic model AIOMFAC: calculation of activity coefficients for organic-inorganic mixtures containing carboxyl, hydroxyl, carbonyl, ether, ester, alkenyl, alkyl, and aromatic functional groups, *Atmos. Chem. Phys.*, 2011, **11**, 9155–9206.

57 A. Zuend, C. Marcolli, T. Peter and J. H. Seinfeld, Computation of liquid-liquid equilibria and phase stabilities: implications for RH-dependent gas/particle partitioning of organic-inorganic aerosols, *Atmos. Chem. Phys.*, 2010, **10**, 7795–7820.

58 A. Zuend and J. H. Seinfeld, A practical method for the calculation of liquid–liquid equilibria in multicomponent organic–water–electrolyte systems using physicochemical constraints, *Fluid Phase Equilib.*, 2013, **337**, 201–213.

59 M. D. Petters and S. M. Kreidenweis, A single parameter representation of hygroscopic growth and cloud condensation nucleus activity, *Atmos. Chem. Phys.*, 2007, **7**, 1961–1971.

60 T. Kent, Water content of latent fingerprints–Dispelling the myth, *Forensic Sci. Int.*, 2016, **266**, 134–138.

61 J. C. Wu, *Statistical analysis of widths and heights of fingerprint images in terms of ages from segmentation data*, 2008, https://www.nist.gov/system/files/finger_size_age.pdf.

62 G. Bekö, P. Wargocki, N. Wang, M. Li, C. J. Weschler, G. Morrison, S. Langer, L. Ernle, D. Licina and S. Yang, The Indoor Chemical Human Emissions and Reactivity (ICHEAR) project: Overview of experimental methodology and preliminary results, *Indoor Air*, 2020, **30**, 1213–1228.

63 T. Berkemeier, M. Ammann, U. K. Krieger, T. Peter, P. Spichtinger, U. Pöschl, M. Shiraiwa and A. J. Huisman, Technical note: Monte Carlo genetic algorithm (MCGA) for model analysis of multiphase chemical kinetics to determine transport and reaction rate coefficients using multiple experimental data sets, *Atmos. Chem. Phys.*, 2017, **17**, 8021–8029.

64 S. Zhou, B. C. Hwang, P. S. Lakey, A. Zuend, J. P. Abbatt and M. Shiraiwa, Multiphase reactivity of polycyclic aromatic hydrocarbons is driven by phase separation and diffusion

© 2023 The Author(s). Published by the Royal Society of Chemistry

Environ. Sci.: Atmos., 2023, **3**, 49–64 | **63**

limitations, *Proc. Natl. Acad. Sci. U. S. A.*, 2019, **116**, 11658–11663.

65 A. C. Vander Wall, P. S. J. Lakey, E. Rossich Molina, V. Perraud, L. M. Wingen, J. Xu, D. Soulsby, R. B. Gerber, M. Shiraiwa and B. J. Finlayson-Pitts, Understanding interactions of organic nitrates with the surface and bulk of organic films: implications for particle growth in the atmosphere, *Environ. Sci.: Processes Impacts*, 2018, **20**, 1593–1610.

66 S. Xu, F. Mahrt, F. K. Gregson and A. K. Bertram, Possible Effects of Ozone Chemistry on the Phase Behavior of Skin Oil and Cooking Oil Films and Particles Indoors, *ACS Earth Space Chem.*, 2022, **6**, 1836–1845.

67 A. T. Slominski, M. A. Zmijewski, C. Skobowiat, B. Zbytek, R. M. Slominski and J. D. Steketee, in *Sensing the Environment: Regulation of Local and Global Homeostasis by the Skin's Neuroendocrine System*, Springer, 2012, pp. 7–26.

68 E. Proksch, pH in nature, humans and skin, *J. Dermatol.*, 2018, **45**, 1044–1052.

69 G. Kortüm, W. Vogel and K. Andrussow, Dissociation constants of organic acids in aqueous solution, *Pure Appl. Chem.*, 1960, **1**, 187–536.

70 J. A. Dean, *Handbook of Organic Chemistry*, McGraw-Hill New York, New York, NY, 1987.

71 C. Wang, D. B. Collins, C. Arata, A. H. Goldstein, J. M. Mattila, D. K. Farmer, L. Ampollini, P. F. DeCarlo, A. Novoselac and M. E. Vance, Surface reservoirs dominate dynamic gas-surface partitioning of many indoor air constituents, *Sci. Adv.*, 2020, **6**, eaay8973.

72 R. Sheu, C. F. Fortenberry, M. J. Walker, A. Eftekhari, C. Stönner, A. Bakker, J. Peccia, J. Williams, G. C. Morrison and B. J. Williams, Evaluating Indoor Air Chemical Diversity, Indoor-to-Outdoor Emissions, and Surface Reservoirs Using High-Resolution Mass Spectrometry, *Environ. Sci. Technol.*, 2021, **55**, 10255–10267.

73 S. M. Duncan, S. Tomaz, G. Morrison, M. Webb, J. Atkin, J. D. Surratt and B. J. Turpin, Dynamics of residential water-soluble organic gases: Insights into sources and sinks, *Environ. Sci. Technol.*, 2019, **53**, 1812–1821.

74 H. Schwartz-Narbonne, J. P. Abbatt, P. F. DeCarlo, D. K. Farmer, J. M. Mattila, C. Wang, D. J. Donaldson and J. A. Siegel, Modeling the Removal of Water-Soluble Trace Gases from Indoor Air *via* Air Conditioner Condensate, *Environ. Sci. Technol.*, 2021, **55**, 10987–10993.

75 E. S. Frank, H. Fan, M. Shrestha, S. Riahi, D. J. Tobias and V. H. Grassian, Impact of adsorbed water on the interaction of limonene with hydroxylated SiO_2: implications of π-hydrogen bonding for surfaces in humid environments, *J. Phys. Chem. A*, 2020, **124**, 10592–10599.

76 B. E. Cummings, Y. Li, P. F. DeCarlo, M. Shiraiwa and M. S. Waring, Indoor aerosol water content and phase state in US residences: impacts of relative humidity, aerosol mass and composition, and mechanical system operation, *Environ. Sci.: Processes Impacts*, 2020, **22**, 2031–2057.

77 J. L. Nguyen, J. Schwartz and D. W. Dockery, The relationship between indoor and outdoor temperature, apparent temperature, relative humidity, and absolute humidity, *Indoor Air*, 2014, **24**, 103–112.

78 D. Rim, E. T. Gall, S. Ananth and Y. Won, Ozone reaction with human surfaces: Influences of surface reaction probability and indoor air flow condition, *Build Environ.*, 2018, **130**, 40–48.

79 Y. Liu, P. K. Misztal, C. Arata, C. J. Weschler, W. W. Nazaroff and A. H. Goldstein, Observing ozone chemistry in an occupied residence, *Proc. Natl. Acad. Sci. U. S. A.*, 2021, **118**, e2018140118.

80 N. Zannoni, P. S. J. Lakey, Y. Won, M. Shiraiwa, D. Rim, C. J. Weschler, N. Wang, L. Ernle, M. Li, G. Bekö, P. Wargocki and J. Williams, The human oxidation field, *Science*, 2022, **377**, 1071–1077.

81 S. Zhou, B. C. H. Hwang, P. S. J. Lakey, A. Zuend, J. P. D. Abbatt and M. Shiraiwa, Multiphase reactivity of polycyclic aromatic hydrocarbons is driven by phase separation and diffusion limitations, *Proc. Natl. Acad. Sci. U. S. A.*, 2019, **116**, 11658–11663.

82 S. Xu, F. Mahrt, F. K. A. Gregson and A. K. Bertram, Possible Effects of Ozone Chemistry on the Phase Behavior of Skin Oil and Cooking Oil Films and Particles Indoors, *ACS Earth Space Chem.*, 2022, **6**, 1836–1845.

83 M. Yao, P. S. J. Lakey, M. Shiraiwa and B. Zhao, Volatile products generated from reactions between ozone and human skin lipids: A modelling estimation, *Build Environ.*, 2022, **217**, 109068.